Available online at www.sciencedirect.com
ScienceDirect
Journal of Theoretical Biology 248 (2007) 340–349
Journal of Theoretical Biology
www.elsevier.com/locate/yjtbi

Incorporating toxin hypothesis into a mathematical model of persister formation and dynamics

N.G. Cogan*

Department of Mathematics, Tallahassee, FL 32306, USA

Received 6 February 2007; received in revised form 16 May 2007; accepted 16 May 2007
Available online 26 May 2007

Abstract

Biofilms are well known for their extreme tolerance to antibiotics. Recent experimental evidence has indicated the existence of a small fraction of specialized persister cells may be responsible for this tolerance. Although persister cells seem to exist in planktonic bacterial populations, within a biofilm the additional protection offered by the polymeric matrix allows persister cells to evade elimination and serve as a source for re-population.

Whether persister cells develop through interactions with toxin/antitoxin modules or are senescent bacteria is an open question. In this investigation we contrast results of the analysis of a mathematical model of the toxin/antitoxin hypothesis for bacteria in a chemostat with results incorporating the senescence hypothesis. We find that the persister fraction of the population as a function of washout rate provides a viable distinction between the two hypotheses.

We also give simulation results that indicate that a strategy of alternating dose/withdrawal disinfection can be effective in clearing the entire persister and susceptible populations of bacteria. This strategy was considered previously in analysis of a generic model of persister formation. We find that extending the model of persister formation to include the toxin/antitoxin interactions in a chemostat does not alter the qualitative results that success of the dosing strategy depends on the withdrawal time.

While this treatment is restricted to planktonic bacterial populations, it serves as a framework for including persister cells in a spatially dependent biofilm model.

Keywords: Biofilm; Mathematical model; Senescence; Dose response; Tolerance; Sensitivity

1. Introduction

Bacteria often grow in biofilms, which are thin aggregates of microorganisms that form on and coat various surfaces. Biofilms are known to be the source of many diseases and microbial infections as well as industrial fouling and corrosion (Coetser and Cloete, 2005; Costerton, 2001). Biofilms are responsible for typical health issues such as urinary tract infections and dental plaque but are also responsible for more lethal medical conditions such as endocarditis and cystic fibrosis (Lindsay and von Holy, 2006).

Antibiotics are commonly used to eliminate bacterial infections in clinical settings; however, bacteria existing in a biofilm setting are remarkably difficult to eliminate (Davies, 2003). There are many sources of biofilm tolerance that are currently being explored. The biofilm structure can prevent an applied antimicrobial agent from reaching the entire bacterial population by mechanisms such as neutralizing reaction with components of the biofilm, synthesis of an antimicrobial degrading enzyme, adsorption of the antimicrobial by the exo-polymeric substance (EPS) or simply not allowing penetration into the biofilm (Lappin-Scott and Costerton, 1995; Stewart, 1996).

It has also been suggested that varying growth rates give rise to a physiological mechanism for biofilm tolerance (Desai et al., 1998; Sufya et al., 2003). The variation in growth rates may be due to intrinsic variation in the

*Tel.: +1 850 644 7196; fax: +1 850 644 4053.
E-mail address: cogan@math.fsu.edu

0022-5193/$ - see front matter © 2007 Elsevier Ltd. All rights reserved.
doi:10.1016/j.jtbi.2007.05.021

bacteria or due to pockets of nutrient depletion. In either case, because antibiotics are typically less effective against slowly growing bacteria, variations in the growth rate may allow some of the population to evade elimination.

An alternative explanation of biofilm tolerance is that a small fraction of the population may exhibit a 'persister' phenotype, that is immune to antibiotic treatment (Balaban et al., 2005; Lewis, 2001). The persister fraction is not eliminated by the antibiotic and can reproduce once the conditions within the biofilm change.

Mathematical models and analysis have been used to understand the interaction between bacteria and their environment. Mathematical analysis of various resistance mechanisms has been successful in indicating that physiological and structural tolerance mechanisms do not fully explain the observed tolerance (Cogan and Keener, 2004; Grobe et al., 2002; Sanderson and Stewart, 1997; Dodds et al., 2000; Roberts and Stewart, 2004). Therefore, recent mathematical models have begun to incorporate persister formation (Cogan, 2006; Chambliss et al., 2006; Roberts and Stewart, 2005; Klapper et al., 2006).

In Cogan (2006), the mechanism of persister formation was only qualitatively included. We assumed that the transition rate from susceptible to persister depended only on the growth rate. The main results of the analysis indicated that persisters can be eliminated by an alternating dosing strategy. Recently, more detailed biological understanding has been described (Lewis, 2005; Shah et al., 2006; Korch and Hill, 2006) where it is shown that overproduction of toxin molecules, such as *RelE* or *HipA*, produces an increase in the persister population. Both *RelE* and *HipA* inhibit the target of the antibiotic, rendering the bacterium immune to the therapy. Therefore, to understand the dynamics of persister formation, the dynamics of the toxin molecules must be specified.

It should be noted that this is not the only hypothesis concerning persister formation. Recent experimental evidence suggests that both symmetric and asymmetric cell division can give rise to variations in bacterial populations that reflect aspects of persistence (Ackerman et al., 2003; Stewart et al., 2005). The hypothesis that persister cells are senescent bacteria was incorporated into a mathematical model Klapper et al. (2006). Analysis of the model indicates that this hypothesis is consistent with observed dynamics.

One of the aims of this investigation is to incorporate a more detailed mechanism for persister formation as described in (Lewis, 2005) into a mathematical model. This extends the results from our previous investigation. However, we will also describe qualitative differences between the predictions of the dynamics of persister populations in a chemostat for the two hypotheses: senescence and toxin production. This difference provides a simple experimental procedure to distinguish the two hypotheses.

In the following sections we describe the components of the model system. First, some background is provided for each of the constituents. We then briefly review our previous model and notation as well as the extensions that have been made. The mathematical model for the chemostat system is derived and analyzed. Finally the results and future directions are discussed.

2. Model system

We assume that there are two main states for bacteria:

- Susceptible: These are bacteria which reproduce and are vulnerable to antibiotic treatment.
- Persisters: These are bacteria whose reproduction is inhibited by the antibiotic. In a previous investigation (Cogan, 2006), we allowed for transition from persister to susceptible phenotype whenever there was no antibiotic; however, in the washout simulations antibiotic will always be present so the persisters are irreversibly formed. We further assume that antibiotic has no other effect on the persister bacteria.

We assume that the transition from susceptible to persister phenotype is governed by a toxin molecule. A typical bacterium produces toxin molecules as well as antitoxin molecules. The toxin is a stable protein that inhibits reproduction while the antitoxin is an unstable protein that forms an inert complex with the toxin protein. It has been suggested that toxins are produced as a stress—response to allow the bacterium to survive unfavorable growth conditions (Chang et al., 2002; Hazan et al., 2004). Our main assumption is that susceptible bacteria produce toxins at a rate that is inversely related to the nutrient concentration with a bounded maximal rate. Although this neglects many other possible stress-inducers, this seems to be a warranted assumption in a wide variety of systems (Pandey and Gerdes, 2005; Brown and Shaw, 2003). The antitoxin production is assumed to be constant throughout the susceptible population.

The mechanism of persister formation that we incorporate in this investigation is a simplification of that suggested in Lewis (2001). Susceptible bacteria in the population produce stable toxin which can bind to a target protein within a susceptible bacteria. Once the toxin has bound to the target, the bacteria becomes a persister and is insensitive to antibiotics. We also assume that the binding to the target, while reversible in general, is *not* reversible when there is antibiotic present. In general, this assumption is valid within the context of the model since the dose–response curves shown in experimental investigations for long-term antibiotic application indicate that the persister population is stable for extremely long times (Keren et al., 2004; Desai et al., 1998). This implies that if the toxin binding induces persister formation, the binding is essentially irreversible in the presence of antibiotic.

At the same time, bacteria produce antitoxin which is unstable and can form a toxin/antitoxin complex by interacting with the toxin molecule. This complex serves to repress the free toxin in the system. Thus, we are interested in

the dynamics of two populations of bacteria: susceptible (B_s) and persister (B_p), and four constituents: toxin (T), antitoxin (A), toxin/antitoxin (TA) and nutrient (C). We do not track TA explicitly since it is not needed for the bacterial dynamics.

We also chose to analyze the dynamics of the system in a chemostat system, with washout rate τ, rather than batch culture. Models in chemostat systems have the advantage that non-trivial steady-states can be investigated. In particular, we will focus on the ratio of the persister population to the total population as a function of the parameters. We show that the most important parameter is the washout rate and that as the washout rate increases the fraction of the population that exhibits persister phenotype decreases. This accords with results from other models (Klapper et al., 2006); however, the time scales are substantially different. This difference provides a method to differentiate between hypothetical mechanisms of persister formation. We note that batch culture results are obtained by setting the washout rate, τ, to zero.

3. Chemostat model

In this section we describe the components of the model. We first isolate the toxin/antitoxin component to derive the transition rate in terms of the bacterial population and the nutrient level. We then specify the mathematical model for the dynamics of a susceptible and persister population model. Throughout, we are neglecting any spatial component to the model and describe only the ODEs (in time) that determine the various populations.

3.1. Toxin, antitoxin module

Toxin, T, is produced by the susceptible population, B_s, at a rate that is inversely related to the nutrient concentration, C. Thus, toxin production is an indication of starvation stress response alone. In the absence of experimental data indicating the functional relationship between toxin production and environmental stress, we posit a qualitatively reasonable relationship. We assume that the rate of production is bounded above by k_t, when the nutrient level is zero and decreases as C increases. Following the argument in Lewis (2005), we further assume that the toxin is stable but can combine with antitoxin, A, to form a complex at rate r^+. The complex is assumed to be stable and is not explicitly needed. The antitoxin is produced by the susceptible population at a constant rate k_a. The antitoxin is unstable and degrades at a rate γ. For the dynamics in a chemostat the toxin and antitoxin washout at a rate τ. The equations governing the concentration of the toxin and antitoxin are

$$\frac{dT}{dt} = \frac{k_t}{1+C} B_s - r^+ TA - \tau T, \tag{1}$$

$$\frac{dA}{dt} = k_a B_s - r^+ TA - \gamma A - \tau A. \tag{2}$$

4. Bacteria and nutrient dynamics

To determine the dynamics of the population we derive dynamics equations governing the susceptible population, B_s (cfu), the persister population, B_p (cfu) and the nutrient concentration, C (kg/m^3). The transition from susceptible type to persister type is assumed to be proportional to the concentration of free toxin, T. The reversion from persister to susceptible is assumed to occur at a constant rate that is small compared to the forward transition rate. Experiments have suggested that, in the presence of antibiotic challenge, the transition rate may be close to zero (Keren et al., 2004; Desai et al., 1998). For the constant dosing experiments we set this parameter to zero; however, this parameter cannot be neglected entirely when considering the dynamics for alternating dosing as this serves as the source for population regrowth. We assume that susceptible types grow at a rate that is proportional to the nutrient concentration. The proportionality constant is denoted αY, where α is the intrinsic growth rate and Y denotes the yield fraction. Although other growth rates are possible (e.g. saturating), this assumption is made so that the comparisons with simulations in Klapper et al. (2006) are valid. Finally, the susceptible population is killed at a rate d that, in general, depends on the antibiotic and the corresponding concentration although here we do not address differences in the outcomes for various antibiotics. In particular, $d = 0$ if there is no antibiotic challenge. Putting these assumptions together yields the following system of equations:

$$\frac{dB_s}{dt} = \alpha Y C B_s - d B_s - k_+ T B_s + k_- B_p - \tau B_s, \tag{3}$$

$$\frac{dB_p}{dt} = k_+ T B_s - k_- B_p - \tau B_p, \tag{4}$$

$$\frac{dC}{dt} = -\alpha C B_s + \tau (C_0 - C). \tag{5}$$

Eqs. (1)–(5) govern the dynamics of the chemostat system. Typical parameters used in the simulations are shown in Table 1. We note that the growth rate and yield coefficients were chosen as in Klapper et al. (2006), the

Table 1
Parameters and ranges of values used in the simulations

Parameter	Value
α	$1 \times 10^{-5}\,\mathrm{h}^{-1}\,\mathrm{cfu}^{-1}$
Y	1.3×10^5 cfu m^3/kg
d	$25\,\mathrm{h}^{-1}$
k_+	$0.005\,\mathrm{h}^{-1}$
k_-	0 or $10^{-6}\,\mathrm{h}^{-1}$
k_t	$0.01-1.0\,\mathrm{h}^{-1}$
k_a	$0.01-1.0\,\mathrm{h}^{-1}$
r_+	$0.01-1.0\,\mathrm{h}^{-1}$
C_0	$1\,\mathrm{kg/m}^3$
γ	$0.001-1.0\,\mathrm{h}^{-1}$
τ	$0-50\,\mathrm{h}^{-1}$

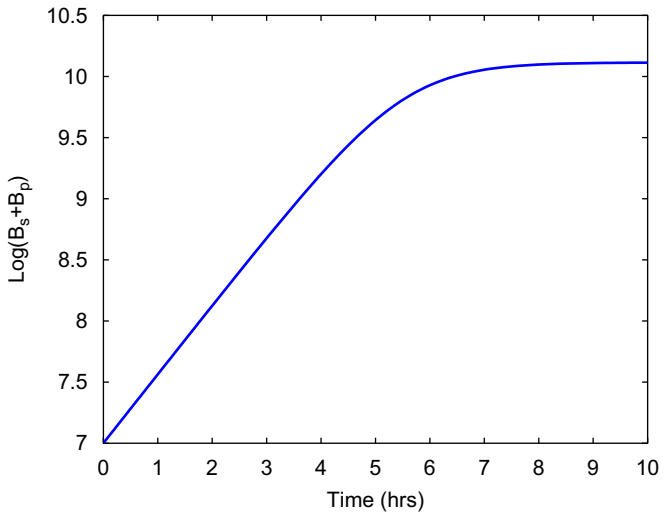

Fig. 1. The growth curve for an unchallenged population with no washout. The parameters for this simulation were: $\alpha = 10^{-5}\,h^{-1}\,cfu^{-1}$, $Y = 1.3 \times 10^5$ cfu m^3/kg, $d = 0\,h^{-1}$, $k_+ = 0.005\,h^{-1}$, $k_- = 1 \times 10^{-6}$, $k_t = 0.25\,h^{-1}$, $k_a = 0.5\,h^{-1}$ and $r_+ = 0.5\,h^{-1}$.

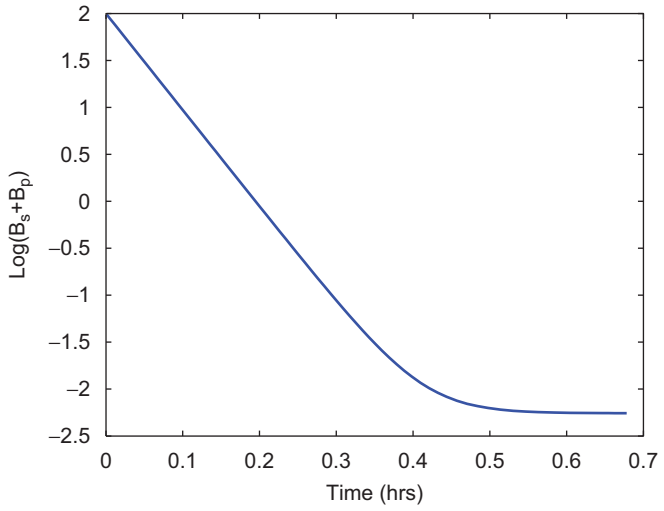

Fig. 2. The growth curve for an unchallenged population with no washout. The parameters for this simulation were the same as those in Fig. 1 except for the disinfection rate which was $d = 25\,h^{-1}$.

forward and backward transition rates k_+ and k_- were chosen so that the batch culture results were similar to those described in Keren et al. (2004). In particular, we chose the rates so that the time scale for decay of the population during constant challenge was in the order of 0.5 h and the population of persisters was comparable to the experimental values (see Figs. 1 and 2). The substrate source concentration, C_0, was fixed to a representative value. The other parameters, k_t, k_a and r_+, are not available, so we tested the model for a wide range of values. For all simulations, except those noted, we solve the governing system of equations using a fourth-order Runga–Kutta algorithm. For the washout simulations, the dynamics were simulated until the system approached a numerical steady-state.

One of the purposes of this investigation is to determine a viable measurement that can distinguish between to possible mechanisms of persister formation: senescence and toxin/antitoxin mediation. For that reason, the kinetics of our model are chosen to match those in Klapper et al. (2006) where this is possible (e.g. growth kinetics). We have also fixed particular forms for the kinetics of the toxin and antitoxin dynamics that are motivated by qualitative assumptions. To better understand the relationship between the parameters and the results, we performed sensitivity and uncertainty analysis. The details are described below, but the outcome indicates that there is a difference in the time scale of persister washout predicted by the senescence and toxin models. This distinction indicates a possible experimental measurement to distinguish the two mechanisms.

We first show that for representative values of the parameters, the unchallenged growth curves and the constant dosing growth curves are similar to those determined experimentally. These curves were generated with no washout, corresponding to batch culture as in the experiments. We view these results as validation that the parameter values are in realistic ranges. We see that the time scale for the decay of the population during constant challenge is in the order of 0.5 h. Also, the persister population is similar to that in the experiments and previous mathematical investigations (Cogan, 2006; Keren et al., 2004).

5. Results

5.1. Chemostat

In this section we concentrate on the steady-state behavior in a chemostat. In Klapper et al. (2006), the authors formulate a model of persister formation incorporates the hypothesis that bacterial senescence governs the formation of persisters. The chemostat model is analyzed and the persister fraction at steady-state is determined as a function of the washout rate, τ. Qualitatively, it is shown that the persister fraction is monotonically decreasing in τ. In particular, when τ is less than approximately 10^{-2}, the persisters compose the entire population of bacteria. For larger values of τ there is an abrupt decrease in persister fraction. At approximately $\tau = 10^{-1/2}$, the persister fraction is also eliminated.

One of the goals of the current investigation is to provide a distinction between two hypotheses of persister formation, senescence and toxin-regulated formation. To that end, we analyze our model for varying washout rates, τ (see Fig. 3).

Qualitatively, we see a similar behavior to that in Klapper et al. (2006); however, the time-scale for the removal of the persister fraction is delayed. In particular, for a wide range of parameters, we see that the toxin/antitoxin

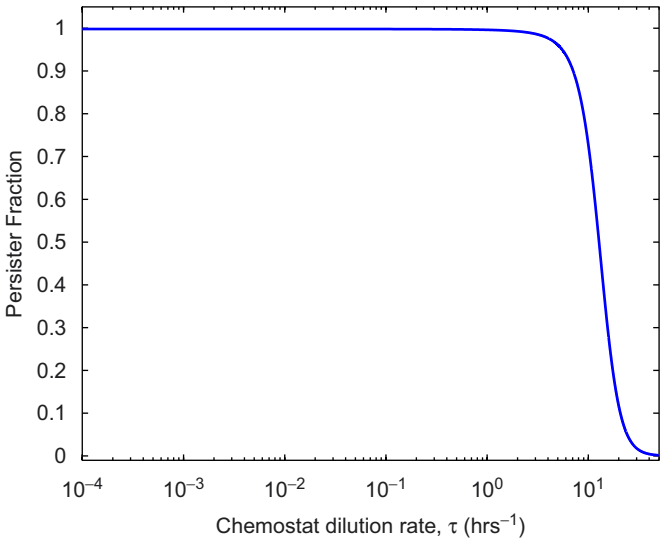

Fig. 3. Persister fraction as a function of the washout rate τ. Here we see that for very low values of τ the entire population in the chemostat is of persister type, which agrees with batch culture results. As the washout rate increases we see an abrupt decrease in the persister fraction indicating that the persisters are accounting for less of the total population. For this simulation $k_t = 0.25$, $k_a = 0.25$ and $r_+ = 0.05$.

Table 2
The LHS table generated by randomly sampling an equi-probable discretization of the probability distribution of the parameters

Run	k_+	k_t	k_a	r_+	γ
1	0.9683	0.9868	0.5877	0.0502	0.0959
2	0.3837	0.0309	0.0694	0.2382	0.0375
3	0.3200	0.4536	0.3700	0.3912	0.0321
4	0.6336	0.3601	0.0410	0.8066	0.0624
5	0.7054	0.4829	0.8781	0.4765	0.0731
6	0.5828	0.3215	0.5079	0.6226	0.0554
7	0.1437	0.8940	0.3114	0.6617	0.0117
8	0.1071	0.5216	0.6174	0.8927	0.0081
9	0.1957	0.1427	0.2777	0.2990	0.0160
10	0.2446	0.8046	0.9245	0.9729	0.0232
11	0.0314	0.7702	0.4510	0.1564	0.0013
12	0.4374	0.7277	0.1880	0.9083	0.0430
13	0.2972	0.6255	0.1253	0.5481	0.0276
14	0.7567	0.2853	0.9742	0.1966	0.0773
15	0.8983	0.2385	0.4851	0.7250	0.0877
16	0.5008	0.6591	0.6615	0.4367	0.0498
17	0.9308	0.1040	0.7441	0.6016	0.0917
18	0.6661	0.5919	0.8493	0.7842	0.0670
19	0.5482	0.1977	0.7820	0.0717	0.0516
20	0.8274	0.9413	0.2094	0.3245	0.0821

hypothesis predicts that the persister fraction saturates the bacterial population well beyond $\tau = 10^{-1/2}$. This provides an experimentally verifiable distinction between the two hypotheses.

5.2. Estimation of parameters

To better understand the effect of various parameters we also performed uncertainty and sensitivity analysis of several key parameters. Because we are comparing the results of our washout simulations to those in Klapper et al. (2006), we fix the growth rate, α, yield, Y, disinfection rate, d and nutrient source concentration, C_0, to the values given in Klapper et al. (2006). We then analyzed the effects of the parameters k_+, k_t, k_a, r_+ and γ using methods described in Blower and Dowlatabadi (1994).

Sensitivity analysis indicates how changes in the values of a parameter affect the results of the model while uncertainty analysis assesses the variability of the outcome due to uncertainty in the parameter values. Rather than use a complete exploration of the parameter space, where every combination of values of each of the parameters is used, we use a more efficient method: Latin hypercube sampling (LHS). Here probability distributions are defined for each of the $K = 5$, parameters that are varied. The distributions are stratified into N equi-probable intervals, where N is the number of simulations. For each parameter distribution, one sample from each of the intervals is chosen at random and these N parameters values are paired randomly with the N values of the other parameters.

Variability in the outcome for each of the N simulations is an indication of the uncertainty of the results. In practice, there is an empirically determined minimum ($N > \frac{4}{3}K$) for the number of simulations needed to determine the significance of the uncertainty analysis. For our analysis we fix $N = 20$.

The first task is to form the LHS table that gives the parameter values for each of the N simulations. We are not able to infer any particular form for the forms of the probability distributions for our parameters, so we choose a uniform distribution with ranges between 0.01 and 1 for k_+, k_t, k_a and r_+ while γ ranges between 0.001 and 0.1. The LHS table is an $N \times K$ matrix shown in Table 2.

Once the LHS table has been established N simulations are performed using parameter values from each of the rows of the LHS table. Fig. 4 shows the various persister fractions as a functions of the washout rate on a semi-log scale. Although there are clear quantitative differences, in all cases the value of the washout rate, τ, at which the persister fraction declines is clearly much longer than that in Klapper et al. (2006).

We can also determine the sensitivity in the outcome in terms of the variability of the parameters. Again, we follow Blower and Dowlatabadi (1994) and calculate the partial rank correlation coefficient (PRCC). We use a measure of the decline in persister fraction to quantify the outcome of the washout simulations. In particular, we define the washout rate at which the persister fraction is decreasing the fastest (i.e. the inflection point of the washout curves) as τ^* and use this as the outcome variable to compare the simulations.

As noted in Blower and Dowlatabadi (1994), a PRCC value indicates the monotonicity of the input variables (parameters) to the particular outcome variable (τ^*). The sign of the PRCC indicates the qualitative relationship and the magnitude indicates the importance of the uncertainty.

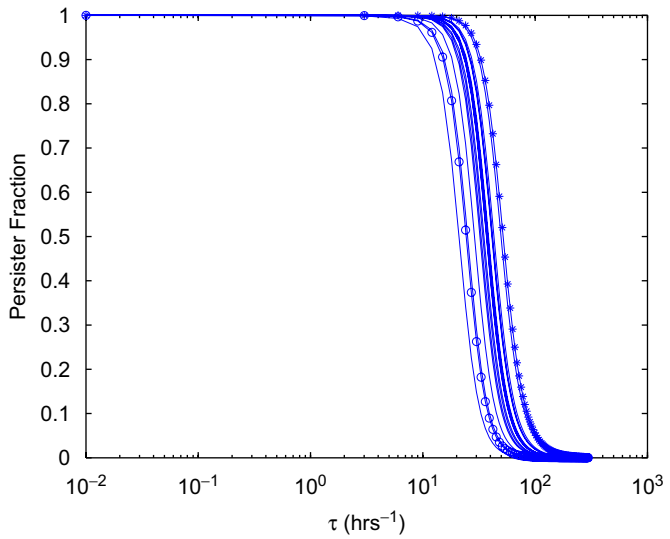

Fig. 4. Comparison of the washout curves for parameters determined by the LHS. We see that the qualitative trend is similar and all the simulations predict persister decline at a much larger value of the washout rate, τ. The simulation with the largest (smallest) value of antitoxin degradation rate, γ, is indicated by $*$ (o).

Table 3
The PRCC values for the varying parameters

Parameter	PRCC
k_+	−0.8235
k_t	−0.5092
k_a	−0.2712
r_+	−0.1933
γ	0.9855

We see that the outcome is most sensitive to the values of k_+ and γ. The sign of the PRCC value indicates the monotonic relationship between the parameter values and the value of the outcome variable.

The details concerning the calculation of the PRCC are given in Blower and Dowlatabadi (1994) and we give a brief description here. We note that an underlying assumption in PRCC is that the outcome is monotonically related to the input parameters, which was verified in this case.

We define a matrix L by augmenting the LHS matrix with the value of the specific outcome variable for each run. A matrix C is defined with elements

$$c_{ij} = \frac{\sum_{t=1}^{N}(l_{it} - (1+N)/2)(l_{jt} - (1+N)/2)}{\sqrt{\sum_{t=1}^{N}(l_{it} - (1+N)/2)^2 \sum_{s=1}^{N}(l_{js} - (1+N)/2)^2}}.$$

The PRCC between the ith input parameter and τ^* is given as

$$PRCC_i = \frac{-b_{i,K+1}}{\sqrt{b_{ii}b_{K+1.K+1}}},$$

where $B = [b_{ij}] = C^{-1}$.

In Table 3 we give the PRCC values for each of the five parameters being tested. We see that all the parameters except for the decay rate of the antitoxin have negative PRCC values. This means that increasing these parameters tends to decrease τ^* while increasing γ tends to increase τ^*. The most sensitive parameters are k_+ and γ. We note that the correlation between increases in γ and τ^* is almost maximal. We see this effect in Fig. 4, where the washout curve corresponding to the set of parameters with the largest and smallest value of γ is indicated.

5.3. Alternating dosing

In this section we describe the results of an alternating dosing protocol on the bacterial population. For the periodic challenge, we introduce two parameters: the dose period, T_d and the withdrawal period, T_w. Antibiotic is applied during T_d, so the reversion from persister to susceptible bacterial types is zero. In Cogan (2006), we handled the transition between dosing and withdrawal in a rather theoretical way by instantaneously removing the antibiotic and replenishing the substrate concentration. Here, we assume that the antibiotic is being introduced as a source to the chemostat during dosing and is being washed out during the withdrawal period. Thus, we append an equation governing the antibiotic concentration, H, to the system introduced above:

$$\frac{dH}{dt} = \tau(H_0 - H), \tag{6}$$

where H_0 denotes the time-dependent concentration of antibiotic being fed into the system. Between the dosing period and the withdrawal period, H_0 is switched between 1 and 0. During T_w, the disinfection rate is assumed to be proportional to the antibiotic concentration. Because the toxin and antitoxin components remain in the system for some time before being washed out we use the values of all the variables at the end of each period T_w and T_d as the initial conditions for the next period.

In Cogan (2006), it was argued that periodic challenge by an antibiotic could be successful in eliminating the persister population. The formation of persisters was linked to the growth rate although no mechanism was described. One can view the current investigation as an extension of the previous model. In particular, we argue that the connection between persister formation and growth rate is governed by the toxin/antitoxin module. Thus, for low nutrient concentration (i.e. low growth rate), there is high production of toxin which subsequently increases the production of persister-type bacteria. In Fig. 5, we show that in batch culture, periodic dosing can be effective in clearing the entire bacterial population when persister formation is regulated by a toxin. As in Cogan (2006) the success depends on the relative period of dose and regrowth. We note that the alternating dose/withdrawal system is inherently non-autonomous and thus difficult to analyze analytically.

In a chemostat with non-zero washout rate, it is no longer clear that this conclusion is the same since the

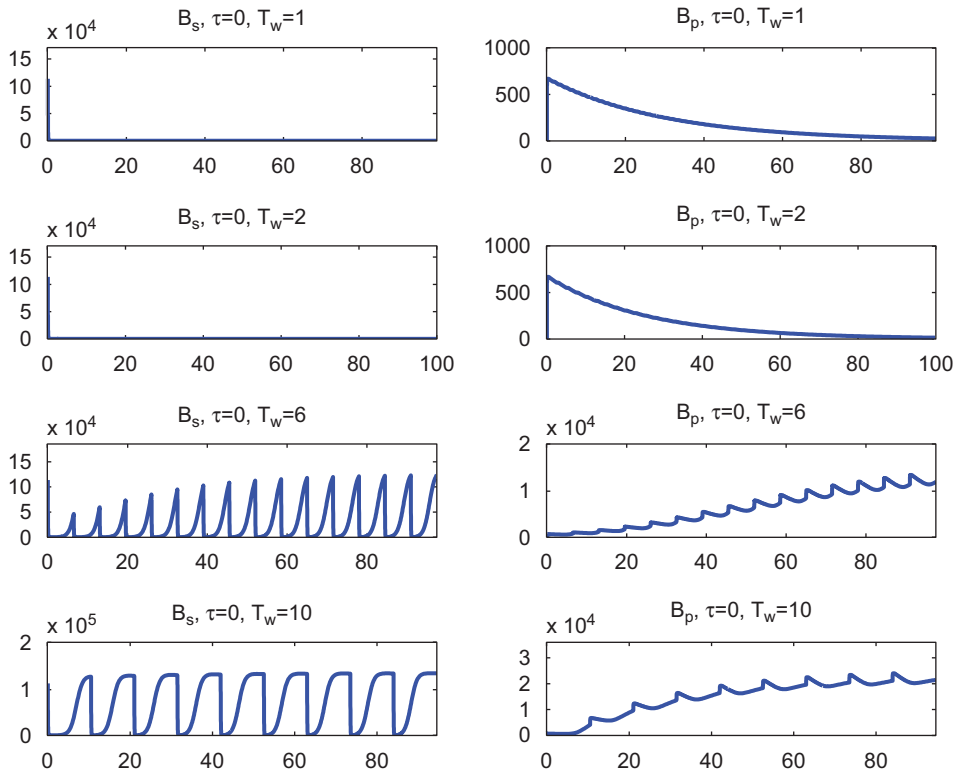

Fig. 5. The batch culture simulation with alternating dosing and withdrawal. Here we follow Cogan (2006) and remove all constituents of the system (e.g. nutrient, antibiotic, toxin and antitoxin) between the dose/withdrawal steps. Here the decay of the population for low values of T_w is not due to washout since $\tau = 0$. But rather it is due to the reversion of persisters to susceptibles, which are then killed during the dosing period.

components of the system are changing dynamically as well as being washed out of the system. We simulated the system varying both the washout rate, τ, and the withdrawal period, T_w, while fixing the dose period at $T_d = 1$. Figs. 6–8 show results of the simulations. In general, we see that if the withdrawal period is very short the persister population remains for some time while if the withdrawal period is too long both susceptible and persister bacteria remain in the system. For intermediate withdrawal times both populations are eliminated. Because the bacteria are constantly being washed away even with no withdrawal the bacteria are all removed; however, rather than being killed they are being washed out. For bacteria within a biofilm this slow removal would not occur, since the bacteria are attached to the surface. Thus, we see that alternating dosing can be effective in a chemostat even when the washout rate is very small as long as the withdrawal period is chosen appropriately. Also, the persister population can be enriched to a periodically varying value as the withdrawal time increases although the magnitude of the persister population declines as the washout rate increases.

5.4. Numerical methods

The simulations detailed above were performed using an explicit Runge–Kutta method. The relative error tolerance was set to 1×10^{-5} and the absolute error tolerance was 1×10^{-6}. Error estimates were obtained using methods described in Dormand and Prince (1980). We also used a variable order Adams–Bashforth–Moulton solver that is part of the ode-suite in MATLAB (ODE113) with the same error tolerance to compare the results.

For typical washout simulation, the l_2-norm of the difference between the persister fractions predicted by the Runge–Kutta and the Adams–Bashforth–Moulton solver is in the order of 10^{-4}. For the alternating dosing simulations, the solutions are given at different times. To compare the results, we interpolate both outputs to common times and compare the l_2-norms of the results. For typical simulations the norm of the difference for all the output variables is less than 10^{-4}.

The agreement between the two solution methods indicates that the results are quite robust.

6. Discussion

In this investigate, we incorporated a simple model of toxin-regulated persister formation in a chemostat. Using numerical methods, we were able to obtain results comparable to experimental results in batch culture. This allowed for estimation of various parameters of the system. We further analyzed the steady-state enrichment of persisters as a function of the washout rate. This contrasts with analysis of alternative hypothesis concerning persister formation. We believe that the contrast, namely the time-scale of persister elimination in a chemostat, provides

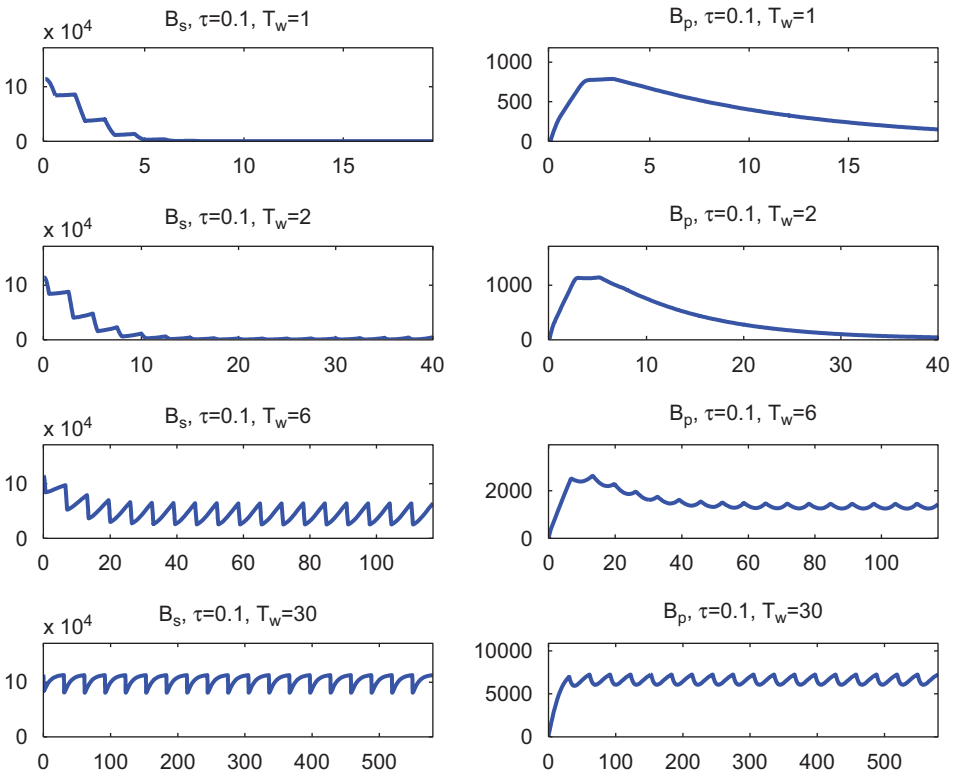

Fig. 6. Chemostat simulation with low washout rate. Here the decay of the persister population for short withdrawal times is actually delayed by the washout. This is slightly non-intuitive, since the washout is decreasing the population of bacteria at each time; however, for low washout rates, the toxin resides in the system delaying the reversion to susceptible.

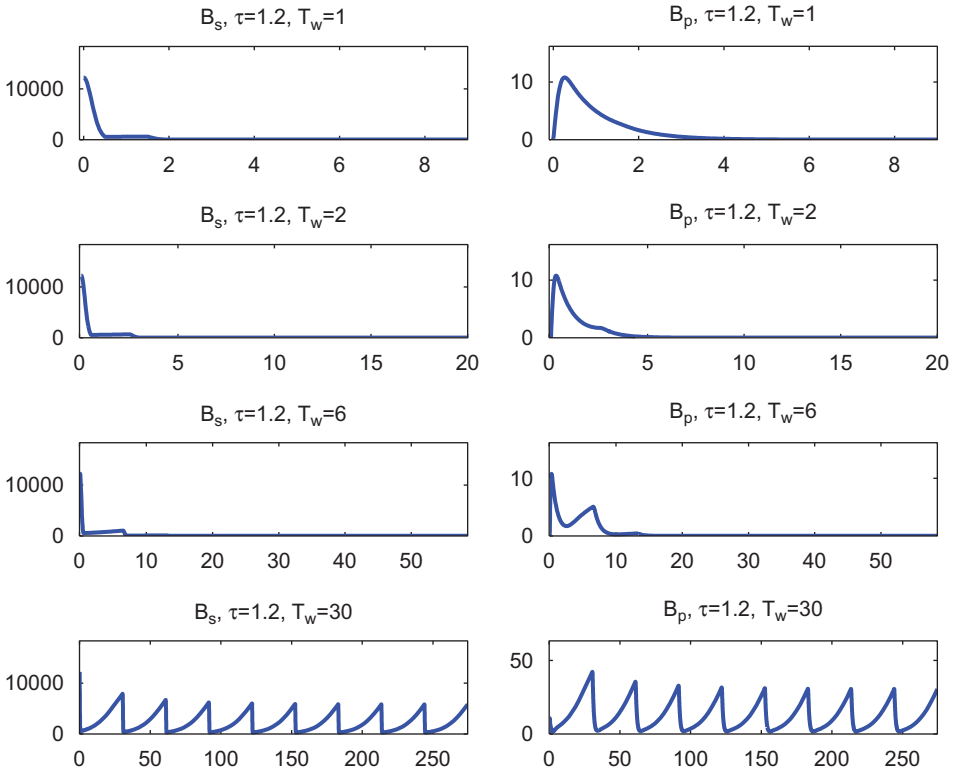

Fig. 7. Chemostat simulation with intermediate washout rate. Shorter withdrawal period slows the elimination of the persister population compared to longer withdrawal periods. However, the increased washout rate increases the effectiveness for short withdrawal periods.

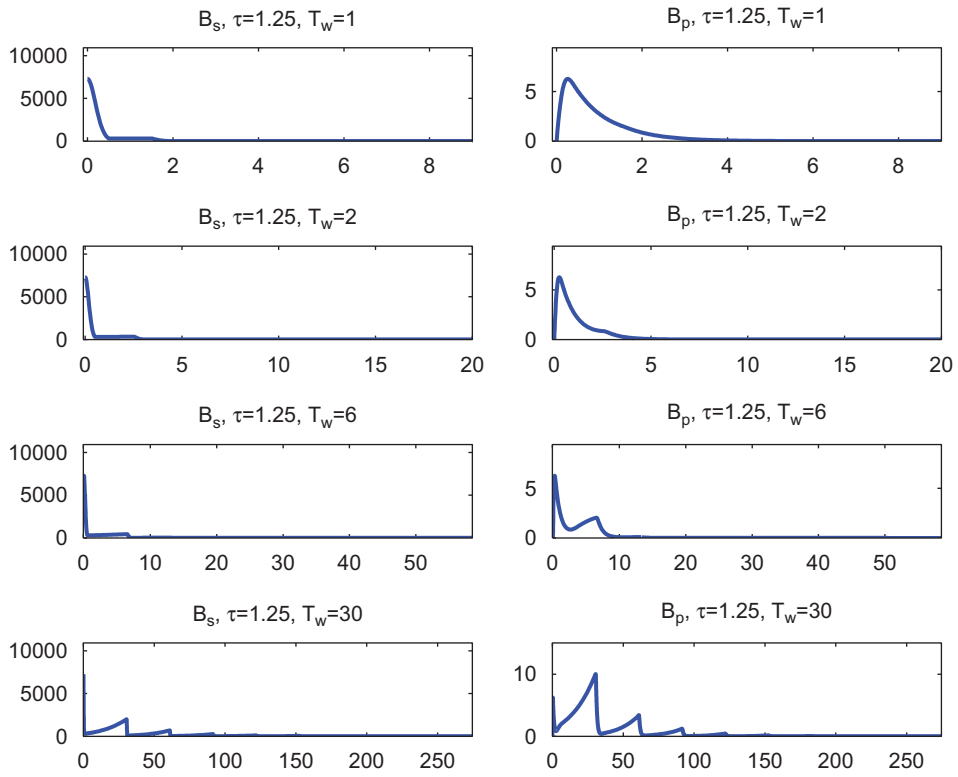

Fig. 8. Chemostat simulation with large washout rate. The washout rate is large enough that the bacteria are being removed from the system relatively quickly unless the withdrawal period is long enough to allow the bacteria to reach a large enough population to withstand removal by both the washout and the antibiotic challenge.

a relatively simple way to distinguish between the reasoning that persister formation is due to senescence or toxin regulation. Because of the intransigence of bacterial populations, especially those growing in a biofilm, understanding mechanisms of tolerance is of paramount importance.

It is becoming increasingly apparent that, while the polymeric component of the biofilm can delay and alter the effectiveness of standard treatments, this does not fully explain bacterial tolerance. Persister formation offers a clear and attractive explanation of the observed tolerance. Therefore, understanding the mechanisms of persister formation becomes one of the aims of current research. Using mathematical analysis to produce possible experimental procedures to distinguish between various hypotheses is itself a useful outcome of mathematical modeling.

We also describe how persister populations, mediated by toxin production, can be eliminated by an alternating dosing strategy. This dosing strategy has been considered in other models Cogan (2006) and experimental situations (Wiuff and Anderson, 2007). It is not at all clear how this will transpire in a biofilm setting since the transport of the nutrients and antibiotics throughout the biofilm is dominated by diffusion. Thus, the interplay between the spatial distribution of bacteria and diffusing constituents in more intricate. However, determining what kinetic behavior is dominant and should be included in spatially distributed systems is important. To that end, the results obtained here indicate that toxin-regulated persister formation is a viable hypothesis that can be included in biofilm settings.

Acknowledgments

The author would like to acknowledge support from NSF award #0612467. This work was also aided by discussions with H. Przychodny.

References

Ackerman, M., Stearns, S.C., Jenal, U., 2003. Senescence in a bacterium with asymmetric division. Science 300, 1920.

Balaban, N.Q., Merrin, J., Chait, R., Kowalik, L., Leibler, S., 2005. Bacterial persistence as a phenotypic switch. Science 305, 1622–1625.

Blower, S.M., Dowlatabadi, H., 1994. Sensitivity and uncertainty analysis of complex models of disease transmission: an HIV model, as an example. Int. Stat. Rev. 62, 229–243.

Brown, J.M., Shaw, K.J., 2003. A novel family of *Escherichia coli* toxin-antitoxin gene pairs. J. Bacteriol. 185, 6600–6608.

Chambliss, J.D., Hunt, S.M., Stewart, P.S., 2006. A three-dimensional computer model of four hypothetical mechanisms protecting biofilms from antimicrobials. Appl. Environ. Microbiol. 72, 2005–2013.

Chang, D.-E., Smalley, D.J., Conway, T., 2002. Gene expression profiling of *Escherichia coli* growth transitions: an expanded stringent response model. Mol. Microbiol. 45, 289–306.

Coetser, S., Cloete, T., 2005. Biofouling and biocorrosion in industrial water systems. Crit. Rev. Microbiol. 31, 213–232.

Cogan, N.G., 2006. Effects of persister formation on bacterial response to dosing. J. Theor. Biol. 238 (3), 694–703.

Cogan, N.G., Keener, J.P., 2004. The role of the biofilm matrix in structural development. Math. Med. Biol. 21, 147–166.

Costerton, J., 2001. Cystic fibrosis pathogenesis and the role of biofilms in persistent infection. Trends Microbiol. 9, 50–52.

Davies, D., 2003. Understanding biofilm resistance to antibacterial agents. Nat. Rev. Drug Discovery 2, 114–122.

Desai, M., Buhler, T., Weller, P., Brown, M., 1998. Increasing resistance of planktonic and biofilm cultures of Burkholderia cepeciax to ciproflaxacin and ceftazidime during exponential growth. J. Antimicrob. Chemother. 42, 153–160.

Dodds, M.G., Grobe, K.J., Stewart, P.S., 2000. Modeling biofilm antimicrobial resistance. Biotechnol. Bioeng. 68, 456–465.

Dormand, J.R., Prince, P.J., 1980. A family of embedded Runge–Kutta formulae. J. Comput. Appl. Math. 6, 19–26.

Grobe, K., Zahler, J., Stewart, P., 2002. Role of dose concentration in biocide efficacy against *Pseudomonas aeruginosa* biofilms. J. Ind. Microbiol. Biotechnol. 29, 10–15.

Hazan, R., Sat, B., Engelberg-Kulka, H., 2004. *Escherichia coli* mazEF-mediated cell death is triggered by various stressful conditions. J. Bacteriol. 186, 3663–3669.

Keren, I., Kaldalu, N., Spoering, A., Wang, Y., Lewis, K., 2004. Persister cells and tolerance to antimicrobials. FEMS Microbiol. Lett. 230, 13–18.

Klapper, I., Gilbert, P., Ayati, B.P., Dockery, J., Stewart, P.S., 2006. Senescence can explain microbial persistence, eprint: q-bio/0610026, ⟨http://adsabs.harvard.edu/as/2006q.bio..10029K⟩.

Korch, S.B., Hill, T.M., 2006. Ectopic overexpression of wild-type and mutant hipa genes in *Escherichia coli*: effects on macromolecular synthesis and persister formation. J. Bacteriol. 188, 3826–3836.

Lappin-Scott, H.M., Costerton, J.W. (Eds.), 1995. In: Mechanisms of the protection of bacterial biofilms from antimicrobial agents. Microbial Biofilms. Cambridge University Press, Cambridge, 1995, pp. 118–130.

Lewis, K., 2001. Riddle of biofilm resistance. Antimicrob. Agents Chemother. 45, 999–1007.

Lewis, K., 2005. Persister cells and the riddle of biofilm survival. Biochemistry (Moscow) 70, 267–285.

Lindsay, D., von Holy, A., 2006. Bacterial biofilms within the clinical setting: what healthcare professionals should know. J. Hosp. Infect. 64, 313–325.

Pandey, D.P., Gerdes, K., 2005. Toxinantitoxin loci are highly abundant in free-living but lost from host-associated prokaryotes. Nucleic Acids Res. 33, 966–976.

Roberts, M.E., Stewart, P.S., 2004. Modeling antibiotic tolerance in biofilms by accounting for nutrient limitation. Antimicrob. Agents Chemother. 48, 48–52.

Roberts, M.E., Stewart, P.S., 2005. Modelling protection from antimicrobial agents in biofilms through the formation of persister cells. Microbiology (UK) 151, 75–80.

Sanderson, S.S., Stewart, P.S., 1997. Evidence of bacterial adaption to monochloramine in *Pseudomonas aeruginosa* biofilms and evaluation of biocide action model. Biotechnol. Bioeng. 56, 201–209.

Shah, D., Zhang, Z., Khodursky, A., Kaldalu, N., Kurg, K., Lewis, K., 2006. Persisters: a distinct physiological state of *E. coli*. BMC Microbiol. 6.

Stewart, E.J., Madden, R., Paul, G., Taddei, F., 2005. Aging and death in an organism that reproduces by morphologically symmetric division. PLoS Biol. 3, e45.

Stewart, P.S., 1996. Theoretical aspects of antibiotic diffusion into microbial biofilms. Antimicrob. Agents Chemother. 40, 2517–2522.

Sufya, N., Allison, D., Gilbert, P., 2003. Clonal variation in maximum specific growth rate and susceptibility towards antimicrobials. J. Appl. Microbiol. 95, 1261–1267.

Wiuff, C., Anderson, D.I., 2007. Antibiotic treatment of in vitro of phenotypically tolerant bacterial populations. J. Antimicrob. Chemother. 59, 254–263.